Available online at www.sciencedirect.com

ScienceDirect

Procedia CIRP 75 (2018) 397–402

www.elsevier.com/locate/procedia

15th CIRP Conference on Computer Aided Tolerancing – CIRP CAT 2018

Highly accurate optical µCMM for measurement of micro holes

Kerstin Zangl[a]*, Reinhard Danzl[a], Franz Helmli[a], Manfred Prantl[a]

[a]Alicona Imaging GmbH, Dr.-Auner-Straße 21a, 8074 Raaba, Austria

* Corresponding author. Tel.: +43 (0) 316 40 30 10 432 ; fax: +43 (0) 316 40 30 10 711. *E-mail address:* kerstin.zangl@alicona.com

Abstract

Highly accurate measurements of small structures are challenging in many applications. An example is the optimization of the hole geometry in fuel injectors. Due to the small size of the structure, tactile approaches are insufficient while standard optical measurement systems cannot provide data on complex geometries. In this paper, a new purely optical 3D micro-coordinate machine – the µCMM of Alicona and its accuracy by determining the maximum permissible translatory and stationary error is presented. Moreover, we demonstrate that the focus variation principle allows 3D measurements of such small components by presenting the measurement and evaluation of micro injection holes.

Peer-review under responsibility of the Scientific Committee of the 15th CIRP Conference on Computer Aided Tolerancing - CIRP CAT 2018.

Keywords: optical 3D micro-coordinate machine (µCMM); focus variation; micro injection hole geometry

1. Introduction

The reduction of manufacturing tolerances, the need to measure small surface details over long distances and the progressive miniaturization in connection with the increasing complexity of industrial components require high-precision 3D measuring instruments for measurements with nm resolution. In addition to complex component geometries, the requirement to measure components independently of the material-related optical properties of plastic, PCD, ceramic, chromium or silicon, which vary from matt to polished or mirrored, is increasing.

In the field of 3D metrology, a large number of measuring instruments for roughness, geometry and form measurement have been developed [1], [2], [3]. In general, the measuring principles of these instruments can be divided into tactile and optical measuring instruments. Tactile measuring instruments enable highly accurate measurements, but are limited in terms of measuring speed, measurement point density and the measurement of complex surface microstructures such as bores due to the contact-based principle.

Optical measuring devices (confocal, white light interferometer, structured light, focus variation) can typically be used only for measurements orthogonal to the surface as they are used for roughness measurement or measurement of small distances. For a detailed overview of coordinate measurement devices, especially µCMMs, we refer to [4], [5].

The presented micro coordinate measurement machine (µCMM) (shown in Fig. 1) is a highly accurate, purely optical, non-contact 3D micro-coordinate measurement machine and enables the measurement of dimensions, position, shape and roughness in one system. The µCMM enables form and geometry measurements as well as profile-based roughness measurements according to ISO 4287 [6] and areal measurements according to ISO 25178 [7]. The measuring principle of the µCMM is based on focus variation [3], [8], [9]. Compared to other optical measuring instruments, it closes the gap between typical 3D coordinate measuring technology and classical surface measuring technology. The focus variation technique combines the low depth of field of an optical system with vertical scanning to obtain topographic and color information from the sample. In addition to the scanned height data, focus variation provides a full depth of field image

2212-8271 © 2018 The Authors. Published by Elsevier B.V.
Peer-review under responsibility of the Scientific Committee of the 15th CIRP Conference on Computer Aided Tolerancing - CIRP CAT 2018.
10.1016/j.procir.2018.05.098

registered to the 3D points. This creates an optical image that eases measurements regarding the identification and localisation of measuring fields or striking surface features. In addition, a new measuring technique enables the measurement of matte as well as highly polished and smooth samples. The new measuring technique is based completely on focus variation but using an advanced illumination method. The illumination of each measurement point is optimized by the use of modulated illumination during the vertical scanning process and the intensity modulation based on a function of time and simultaneously as a function of the lateral position.

Fig. 1. Alicona µCMM - optical 3D micro-coordinate measuring machine.

The measurement of complex microstructures is important in many industrial applications. In this paper we present the micro hole measurement in injection nozzles. Injection systems have a decisive control function in the injection of fuel into the combustion chamber. The optimization of the combustion process by analyzing the influence of the hole geometry of the injector nozzle is an important research topic in the automotive industry.

Current state of the art technology for micro hole measurement focuses on optical measurement systems such as X-ray tomographs [12], [13] and opto-tactile measurement systems using fiber probes [10], [11]. Computer tomographs provide a volume model of the measured component, but are restricted in measurement time and they only are able to measure these holes with relatively low resolution. Tactile-optical coordinate systems based on the fiber probe technology are well known for injection hole measurement. Current measuring systems are limited in terms of the number of measuring points, the problem of accessing holes with diameters in the range of 100µm and the long measuring time. Typically, a fiber probe with a diameter of 80µm and lower is used to measure hole with diameter in the range of 100µm. The measurement of such small geometries with relatively large probes provides a metrological challenge. Because of the contact-based measurement, it is also possible that the fiber breaks, if the real object deviates from the CAD model.

Section 2 gives an overview of the µCMM, its components and technical specifications. Section 3 concentrates on the adjustment and calibration of the µCMM. Finally, in section 4 we demonstrate the 3D measurement of micro injection holes, where the difficulty lies in the highly accurate measurement of steep slopes.

2. Overview of the µCMM

The µCMM is a fixed-bridge coordinate machine [1], [4] with a granite frame, where the x and z axis are constructed as a bridge over the moving y axis. For high accuracy, the system consists of a high-precision air-bearing axis system with linear motors, the optical sensor based on focus variation technology and thermally stable scales made of Zerodur with a resolution of 3.9nm after interpolation and a thermal expansion coefficient of $CTE(0°C; 50°C) = 0 \pm 0.010\ ppm/K$.

In addition, an automatic lens magazine for up to four lenses and an automatic pneumatic lens changer are mounted on the system. This enables a high repeatability of the change process with automatic lens recognition. Optionally, the µCMM can be equipped with a fully automatic tilting and rotating unit. With the µCMM, which is based on the functional principle of focus variation, the following technical specifications result. The µCMM has a total measuring volume of 310 x 310 x 310 mm³ and a traversing speed of the axes of up to 100 mm/s. In addition, it measures up to 1720 x 1720 = 2.95 million measuring points for a single measurement, a measurement of larger areas reaches up to 500 million points. Its vertical resolution depends on the selected lens and can be as good as 3 nm. The vertical measuring range depends on the working distance of the lens and ranges from 4 to 22.5 mm. The lateral measuring range is also determined by the lens used and ranges from 0.13 x 0.13 mm² (using a 100x objective) to 5.2 x 5.2 mm² (using a 2.5x objective) for a single measurement.

3. Accuracy of the µCMM

The correction of geometric errors of the µCMM is done by using a volumetric error compensation. A laser interferometer is used to measure distances in the whole measurement volume of the µCMM. These measurements are repeated several times for each position. With this information, a mathematical model is formulated to correct the raw linear scale position.

The ISO 10360-8[14] and VDI 2617 [15] are used to verify the performance of the instrument. The test uncertainty of the coordinate machine is estimated according to ISO/TS 23165:2006 [16] where the test uncertainty comprises the uncertainty of the material standard of size due to the calibration, the uncertainty due to thermal compensation and the uncertainty of misalignment and fixture of the calibration tool.

The specified measurement uncertainty of the laser interferometer, given by the manufacturer, is $U_{(k=2)} = 0.05\ \mu m + 0.3\mu m/m$ where the uncertainty contributors are the uncertainty of the vacuum wavelength, the interpolation of the interferometer and the uncertainty of pressure, temperature and humidity. The uncertainty due to misalignment and fixture of the material standard of size is assumed to be negligible. Fig. 2 shows the length measurement errors of the laser interferometer. As it can be seen all values are less than the specified maximum permissible unidirectional length error including the test uncertainty of the laser interferometer.

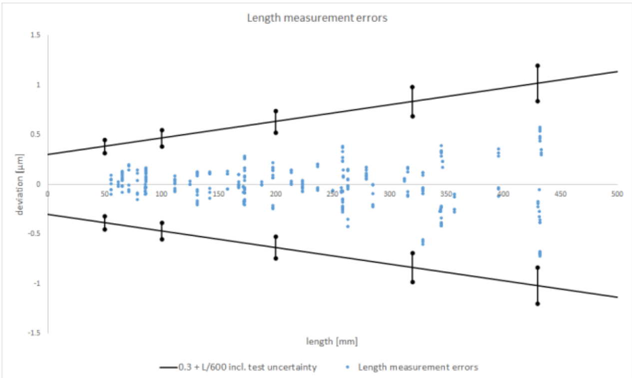

Fig. 2. Length measurement errors of the laser interferometer. The thin black lines shows the MPE for the instrument determined by the laser interferometer. Moreover, the test uncertainty of the laser interferometer is represented graphically according to ISO/TS 23165:2006.

As described in ISO 10360-8 (see chapter B.4.3.4 of ISO 10360-8 for more details), a laser interferometer is used to verify the axis accuracy of the µCMM. The maximum permissible unidirectional length error for the instrument can be specified by

$$E_{Uni:Tr:ODS,MPE} = \left(0.3 + \frac{L}{600}\right) \mu m\ (L\ in\ mm) \qquad (1)$$

where Tr stands for translatory. In addition to the maximum permissible length error, the following maximum permissible unidirectional stationary error is determined by the measurement of height steps in a single field of view

$$E_{UniZ:St:ODS,MPE} = \left(0.15 + \frac{L}{50}\right) \mu m\ (L\ in\ mm) \qquad (2)$$

where St stands for stationary and Z indicates the measurement direction. The probing size error was determined using an advanced calibration artefact (described at the end of this section) and measuring one of the cemented carbide spheres with a calibrated diameter of 1.00124mm (U = 0.20µm). Fig. 3 shows the measured 3D dataset including the sphere fit. The probing size error for this measurement is given by:

$$P_{Size.Sph.All:St:ODS} = 0.12\mu m \qquad (3)$$

where St stands for stationary. The obtained value is actually below the uncertainty of the calibration artefact.

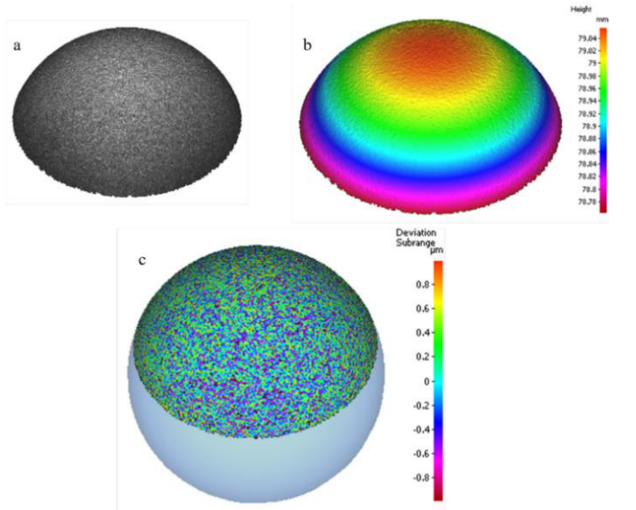

Fig. 3. (a) 3D dataset of the measured sphere surface, (b) 3D dataset in pseudo colour, (c) measured dataset with sphere fit in pseudo colour (with range [-1µm to 1µm]).

The probing form error was determined using a 1mm reference sphere with a calibrated diameter of (1.001 ± 0.02µm) and a calibrated roundness of (0.21 ± 0.04µm). According to ISO 10360-8, for each of the 25 areas a representative point was calculated and the following probing form error was determined

$$P_{Form.Sph.1x25:St:ODS} = 0.405\mu m \qquad (4)$$

According to ISO 10360-8, the bidirectional error can be calculated by considering the measured and calibrated values of unidirectional measurements, the probing form error and the probing size error (see also [17]). By computing the bidirectional errors of all length measurements, the following error was determined between $E_{(Bi:Tr:ODS,MPE)} = (0.585 + L/600)\mu m\ (L\ in\ mm)$ (best case) and $E_{(Bi:Tr:ODS,MPE)} = (0.825 + L/600)\mu m\ (L\ in\ mm)$(worst case).

Additionally, in order to verify the performance of the µCMM according to ISO 10360-8, a ball bar calibration artefact (see Fig. 4) calibrated by the DAkkS (German Accreditation Body) has been developed. The calibration was performed with a 3D CMM Carl Zeiss Prismo using a probe tip with a diameter of 1.5mm and a probe force of 0.2N. The ball bar is made up of Invar which has a very low coefficient of thermal expansion and seven cemented carbide spheres. Details can be found in Table 1. The uncertainty due to misalignment of the calibration artefact lies between 5 and 10 µm. Fig. 5 shows the effect of the misalignment for the measurement of two space diagonals. As it can be seen the length measurement errors of space diagonal 4 are much higher than for space diagonal 1 because the ball bar get out of place during the measurement. Fig. 6 shows length measurement errors measured along the x and y direction. In the first measurement the deviations highly increases between 100 and 300 mm test length. Therefore, the measurement has been repeated by taking care that the ball bar can not move. As it can been seen, in the second measurement all values lies within ±(0.6 + L/600) µm (L in mm). Hence, a revision of the ball bar artifact with regard to the fixation is under progress and consequently a detailed evaluation of the test uncertainty according to ISO/TS 23165:2006 as well as the performance evaluation according to ISO 10360-8 will be future work.

Table 1. Technical specifications of the ball bar calibration artefact

Description	Value
Bar length	400 mm
Sphere diameter	1mm
Sphere distances	0; 10,00267mm; 50,02624mm; 100,03691mm; 199,98865mm; 299,97205mm; 400,01388mm
Coefficient of thermal expansion	1ppm/K
Calibration laboratory	DAkkS
Uncertainty of the sphere center distances	U = (0.12 + L/2500)µm, L in mm

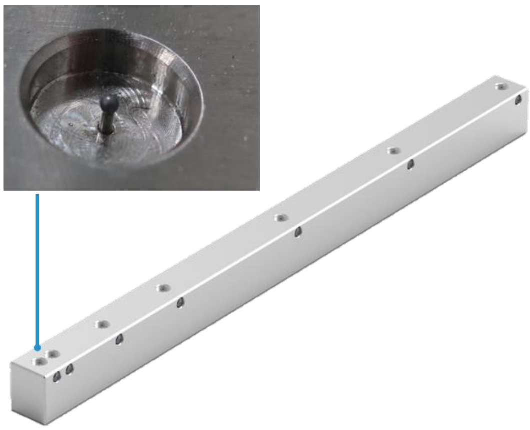

Fig. 4. Ball bar calibration artefact with spheres on the top surface. Moreover, a zoomed in view of one cemented carbide sphere is shown.

In order to measure and verify shorter distances and form measurements, a smaller calibration artefact (see Fig. 7) is used, which consists of sapphire glass and 24 cemented carbide spheres calibrated by the METAS (Federal Institute of Metrology, Switzerland). The calibration has been done by the METAS µ-CMM using a sapphire sphere as probe with a diameter of 0.2 mm and a probing force less than 0.5 mN. Each sphere was probed on its upper half along the equator and along two orthogonal meridians with a point density of 300pts/mm. Details can be found in Table 2. According to ISO/TS 23165:2006 the test uncertainty is specified by the uncertainty due to the calibration of the calibration artifact. The uncertainty due to thermal compensation as well as the uncertainty due to misalignment and fixture of the artifact is assumed to be negligible. Fig. 8 shows the length measurement errors for the lengths between the 1mm spheres on the advanced calibration artefact. The majority of the values lies within ±(0.6 + L/600) µm (L in mm). A detailed analysis of the data has shown that the four outliers are due to an erroneous sphere measurement. Hence, repeated measurements as stated in the ISO 10360-8, would be useful.

Fig. 5. Length measurement errors, measured along space diagonal 1 and 4 (according to ISO 10360-8). Graphical representation of misalignment effect.

Fig. 6. Length measurement errors, measured on the ball bar. The distance of the sphere 2, 3, 4 and 5 to sphere 1 is measured along x and y direction.

Table 2. Technical specifications of the advanced calibration artefact.

Description	Value
Sphere diameters	16x 1mm, 1x 2mm, 7x 0.4mm
Sphere distances	from 0.02 to 57.47mm
Sphere sphericity	from 0.18 to 0.71µm
Coefficient of thermal expansion	8.5ppm/K
Calibration laboratory	METAS
Uncertainty of sphericity	U = 0.22µm
Uncertainty of coordinates and diameter	U = 0.20µm

Fig. 7. Advanced calibration artefact to verify distance and form measurements. The detailed view shows the positions of the 24 cemented carbide spheres.

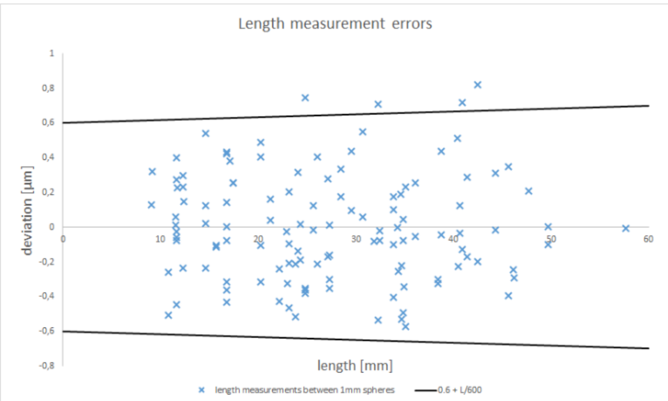

Fig. 8. Length measurement errors, measured between the 1mm spheres of the advanced calibration artefact. The majority of the length measurement errors are less than ±(0.6 + L/600) µm (L in mm).

4. Application - micro hole measurement in fuel injectors

An application, which demonstrates the highly accurate geometric measurement of small and complex components and their geometric relations is the measurement of micro injection holes of valves.

Fig. 9 shows a cross section of such an injection nozzle and the geometry of an injection hole. The relevant parameters are the form as well as orientation with respect to the part axis. In general, the nozzle holes are cylindric (hole inlet diameter = hole exit diameter) or cone-shaped (hole inlet diameter ≠ hole exit diameter). The diameter of these holes is between 120 and 600µm. The diameter to depth ratio of those holes is 1:5. The orientation of a nozzle hole can be described by the angle between the part axis and the hole axis.

Due to the fact, that typically detailed data on injection nozzles are subject to non-disclosure agreements, the measured component is an off-the-shelf part bought in a local car component shop. Therefore, no CAD model or technical drawing of the measured injection nozzles can be presented.

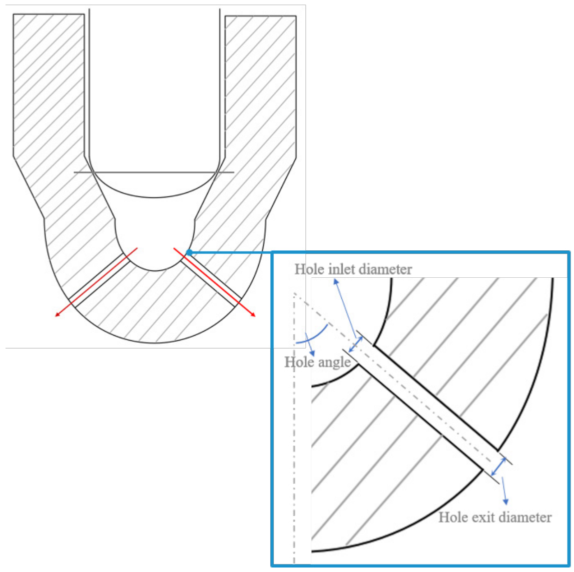

Fig. 9. Cross section of a fuel injector and measured injection hole geometry.

For the measurement of the 3D dataset, the measurement system was equipped with a high-precision rotation unit with calibrated tilting and rotation axis. The injection nozzle is mounted on the motorized rotation unit and the holes are scanned. Due to the depth of field information, a 3D dataset is generated. Fig. 10 shows the resulting 3D dataset of the injection nozzles and the eight measured injection holes. For achieving the geometry parameters, first the hole axis is determined by robustly fitting a cone to the whole geometry. Fig. 11b shows a cross-section through the injection holes. This sectional view clearly shows that the holes are conical. Therefore, a robust cone fit is made in each hole. To determine the bore diameters, a circle is fitted into the cross-section of the inlet and outlet of the bore (see Table 3 and Fig. 10). Here, a standard Gaussian fit with 3σ is used, where all measured points are weighed equally.

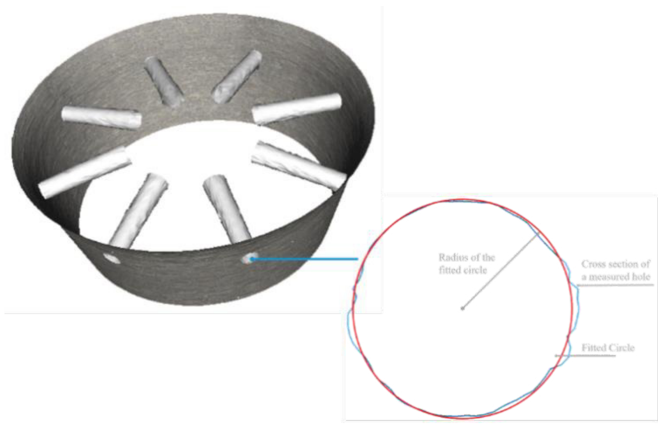

Fig. 10. Measured 3D dataset and measurement of the exit diameter of a hole by fitting a circle in the cross section.

Table 3. Detailed measurement results for one hole.

Hole	Inlet diameter (mm)	Exit diameter (mm)	Cone opening angle (°)
H1	0,1454	0,1255	3,038

In addition to the hole geometry, also the hole angle to the tool axis is evaluated. The tool axis is determined by robustly fitting a cone into the dataset. Afterwards, each angle between the hole axes and the tool axis is computed. Fig. 11a shows a top view of the measured 3D dataset where the individual holes are numbered. In Table 4 the resulting hole angles are summarized.

Table 4. Angle with respect to the outer axis.

Holes	Angle (°)
H1	81,33
H2	81,42
H3	81,35
H4	81,38
H5	81,22
H6	81,33
H7	81,52
H8	81,12

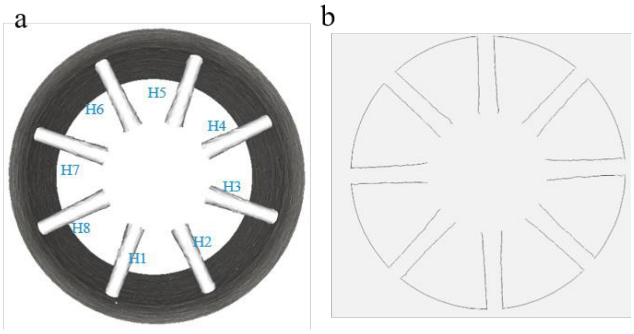

Fig. 11. (a) Top view of the 3D dataset with numbered holes and (b) cross section of the measured holes.

5. Conclusions

Based on the application example of measuring micro holes in a fuel injection nozzle we present an approach for a µCMM based on focus variation. It is shown that the device can successfully determine parameters of such complex micro shapes.
According to ISO 10360-8[14] and VDI 2617 [15] the performance of the instrument has been verified by using a laser interferometer and calibration artifacts calibrated at DAkkS and METAS. Measurements on the calibration artifacts show a maximum permissible length measurement error which is slightly higher than the MPE determined using the laser interferometer which just takes into account the axes accuracy. Therefore, the overall MPE specified by the Alicona in their product specifications is (0.8 + L/600) µm (L in mm) to guarantee the performance for all instruments. Future work needs to be done for the determination of other errors according to ISO 10360-8 not listed in this document as well as the performance evaluation on a revised ball bar artifact. Additionally, it is needed to verify the measurements of the injection holes regarding the uncertainty by a micro hole artifact like the PTB micro hole artifact [18] and a measurement system analysis on the injection nozzle.
Finally, we want to mention, that a revision of the ISO 10360-8 regarding sphere sizes (sphere diameter smaller than 10mm) or probing direction (if instruments cannot measure 90 degree) as well as the work on new standards e.g. the VDI 2617 12.2 [19] would be valuable and necessary.

6. References

[1] Hocken RJ, Pereira P.H. Coordinate Measuring Machines and Systems, 2nd ed. CRC Press 2012
[2] Weckenmann A. Koordinatenmesstechnik – Flexible Strategien für funktions- und fertigungsgerechtes Prüfen, 2nd ed. Hanser Verlag 2012
[3] Leach RK Optical Measurement of Surface Topography. Berlin, Springer-Verlag, 2011
[4] Dai G, Neugebauer M, Stein M, Bütefisch S, Neuschaefer-Rube U. Overview of 3D Micro- and Nanocoordinate Metrology at PTB. App Sci 2016;6:257.
[5] Leach RK. Fundamental Principles of Engineering Nanometrology. 2nd ed., Elsevier, 2014
[6] ISO 4287:1997, Geometrische Produktspezifikation (GPS), Oberflächenbeschaffenheit: Tastschnittverfahren; Norm zur Definition der allgemeinen Rauheitsparameter (Ra, Rq, Rz, ...)
[7] ISO/CD 25178-6:2010, Geometrical product specifications (GPS) - Surface texture: Areal - Part 6: Classification of methods for measuring surface texture.
[8] Danzl R, Helmli F, Scherer S. Focus variation – A robust technology for high resolution optical 3D surface metrology. J Mech Eng, 2011;57:245-56
[9] ISO/CD 25178-606, Geometrical product specification (GPS) – Surface texture: Areal Part 606: Nominal characteristics of non-contact (focus variation) instruments (2015)
[10] Muralikrishnan B, Stone JA, Stoup JR. Fiber deflection probe for small hole metrology, Precis Eng, 2006;30:154-64.
[11] Schwenke H, Wäldele F, Weiskirch C, Kunzmann H. Opto-tactile Sensor for 2D and 3D Measurement of Small Structures on Coordinate Measuring Machines, CIRP Ann, 2001;50:361-4.
[12] Matusik K, Duke D, Swantek A, Powell CF. High resolution X-ray tomography of injection nozzles. In: ILASS–Americas 28th annual conference on liquid atomization and spray systems, Detroit, MI, 15–18 May 2016.
[13] Matusik KE, Duke, DJ, Kastengren AL, Sovis N, Swantek AB, Powell CF. High-resolution X-ray tomography of engine combustion network diesel injectors. Int J Eng Res; 2017
[14] ISO 10360-8:2013 - Geometrical product specifications (GPS) - Acceptance and reverification tests for coordinate measuring systems (CMS) — Part 8: CMMs with optical distance sensors.
[15] VDI/VDE 2617 Blatt 6.2 - Genauigkeit von Koordinatenmessgeräten; Kenngrößen und deren Prüfung; Leitfaden zur Anwendung von DIN EN ISO 10360 für Koordinatenmessgeräte mit optischen Abstandssensoren (in work)
[16] ISO/TS 23165:2006 - Geometrical product specifications (GPS) – Guidelines for the evaluation of coordinate measureing machine (CMM) test uncertainty
[17] Moroni G, Petrò S, Syam WP. Four-axis micro measuring systems performance verification. CIRP Ann - Manuf Technol 2014;63:485-88
[18] Jusko O, Neugebauer M, Wäldele F. Dimensional measuring device calibration body manufacturing method using stack of calibration body blanks of at least 2 different thicknesses provided with required surface contour along one side face. Patent DE 10318762B3; 2004
[19] VDI/VDE 2617 Blatt 12.2 - Genauigkeit von Koordinatenmessgeräten - Kenngrößen und deren Prüfung - Annahme- und Bestätigungsprüfungen für Koordinatenmessgeräte zum optischen Messen von Mikrogeometrienn (project)